J Physiol 589.10 (2011) pp 2625–2639

The Journal of Physiology

Hamstring contractures in children with spastic cerebral palsy result from stiffer extracellular matrix and increased *in vivo* sarcomere length

Lucas R. Smith[1], Ki S. Lee[2], Samuel R. Ward[3], Henry G. Chambers[4] and Richard L. Lieber[1,5,6]

[1]*Departments of Bioengineering,* [3]*Radiology and* [5]*Orthopaedics, University of California, San Diego, CA, USA*
[2]*Department of Orthopaedic Surgery, Severance Children's Hospital, Yonsei University College of Medicine, Seoul, South Korea*
[4]*Department of Orthopaedics, Rady Children's Hospital, San Diego, CA, USA*
[6]*Department of Veterans Affairs Medical Center, San Diego, CA, USA*

Non-technical summary Muscle spasticity, due to an upper motoneuron lesion, often leads to muscle contractures that limit range of motion and cause increased muscle stiffness. However, the elements responsible for this muscle adaption are unknown. Here we show that muscle tissue is stiffer in contracture compared to age-matched children, implicating the extracellular matrix (ECM). However, titin, the major load-bearing protein within muscle fibres, is not altered in contracture, and individual fibre stiffness is unaltered. Increased ECM stiffness is even more functionally significant given our finding of long *in vivo* sarcomeres which leads to much larger *in vivo* forces in muscle contracture. These results may lead to novel therapeutics for treating spastic muscle contracture.

Abstract Cerebral palsy (CP) results from an upper motoneuron (UMN) lesion in the developing brain. Secondary to the UMN lesion, which causes spasticity, is a pathological response by muscle – namely, contracture. However, the elements within muscle that increase passive mechanical stiffness, and therefore result in contracture, are unknown. Using hamstring muscle biopsies from pediatric patients with CP ($n = 33$) and control ($n = 19$) patients we investigated passive mechanical properties at the protein, cellular, tissue and architectural levels to identify the elements responsible for contracture. Titin isoform, the major load-bearing protein within muscle cells, was unaltered in CP. Correspondingly, the passive mechanics of individual muscle fibres were not altered. However, CP muscle bundles, which include fibres in their constituent ECM, were stiffer than control bundles. This corresponded to an increase in collagen content of CP muscles measured by hydroxyproline assay and observed using immunohistochemistry. *In vivo* sarcomere length of CP muscle measured during surgery was significantly longer than that predicted for control muscle. The combination of increased tissue stiffness and increased sarcomere length interact to increase stiffness greatly of the contracture tissue *in vivo*. These findings provide evidence that contracture formation is not the result of stiffening at the cellular level, but stiffening of the ECM with increased collagen and an increase of *in vivo* sarcomere length leading to higher passive stresses.

(Received 2 December 2010; accepted after revision 21 March 2011; first published online 21 March 2011)
Corresponding author R. L. Lieber: Department of Orthopaedic Surgery (0863), UC San Diego and VA Medical Centre, 9500 Gilman Drive, Mail Code 0863, La Jolla, CA 92093-0863, USA. Email: rlieber@ucsd.edu

Abbreviations ACL, anterior cruciate ligament; CP, cerebral palsy; ECM, extracellular matrix; UMN, upper motoneuron.

DOI: 10.1113/jphysiol.2010.203364

Introduction

Cerebral palsy (CP) describes a spectrum of movement disorders caused by upper motoneuron (UMN) lesions that occur in the developing brain (Rosenbaum *et al.* 2007). CP is the most common childhood movement disorder with a prevalence of 3.6 cases per 1000 in the US (Yeargin-Allsopp *et al.* 2008). Although the primary UMN insult is not progressive, the resulting muscle pathology does progress (Kerr Graham & Selber, 2003). Pathological muscle in CP is described as spastic, which is a velocity-dependent resistance to stretch due to reduced inhibition of the stretch reflexes (Crenna, 1998). Despite best clinical practices, children with CP often develop contractures that limit their range of motion, decrease their mobility and may be painful. While muscle spasticity and hyper-activity are commonly seen in cerebral palsy, contracture represents a unique muscle adaptation in which the muscle increases passive stiffness such that range of motion around a joint is limited without active force production of the muscle. Thus, muscle contractures represent a major disability to those affected by CP in particular and those with UMN lesions in general (Bache *et al.* 2003).

The skeletal muscle mechanism by which spasticity results in contracture is not known. Transcriptional data suggest many physiological pathways are altered in contracture (Smith *et al.* 2009). One consistent finding is that spastic muscles from children with CP are weaker than those of typically developing control children due to a combination of decreased neuronal drive, decreased muscle size and decreased specific tension (Elder *et al.* 2003; Rose & McGill, 2005; Stackhouse *et al.* 2005). Previous studies also demonstrated that increased resistance to stretch in spastic muscle has both an active and passive component (Sinkjaer & Magnussen, 1994; Mirbagheri *et al.* 2001; Lorentzen *et al.* 2010). However, the passive elements responsible for this increased stiffness have not been identified and these presumably represent the therapeutic targets of physical therapy (Wiart *et al.* 2008), surgery (Beals, 2001) and neurotoxin injection (Lukban *et al.* 2009). To date, these treatments do not prevent contracture formation (Tilton, 2006).

It should be noted that the term 'contracture' is typically referred to in the muscle physiology literature as an increase in tension of isolated muscles or fibres in response to external activation by caffeine or potassium (Savage & Atanga, 1988). Caffeine induces calcium release from the sarcoplasmic reticulum and potassium depolarizes the muscle as methods to activate the crossbridge cycle that produces muscle active tension (Conway & Sakai, 1960; Hodgkin & Horowicz, 1960). However, the common clinical use of the term 'contracture' does not refer to such activation. Rather, a clinical 'contracture' represents a condition where a muscle becomes extremely stiff, limiting range of motion, perhaps causing pain, and deforming joints. These contractures often result from upper motoneuron lesions such as those that occur after stroke, head injury or cerebral palsy and represent tremendous challenges to treat (O'Dwyer *et al.* 1996; Farmer & James, 2001). Often, clinical contractures result from chronic activation of a muscle, referred to as 'spasticity' and the net result is a stiff muscle that limits the range of motion around a joint in the absence of any active component of crossbridge cycling (Fergusson *et al.* 2007).

As muscle architecture is the most important determinant of muscle force-generating capacity and excursion, previous studies have sought to describe the macroscopic structural adaptation of muscle in CP. It has been suggested that contracture results from shortened muscles and thus multiple studies have used ultrasound technology to measure fascicle length in contractured muscle and, while these experiments confirm reduced CP muscle volume, evidence for shortened fascicles is inconclusive (Shortland *et al.* 2002; Malaiya *et al.* 2007; Mohagheghi *et al.* 2007, 2008). A major drawback of ultrasound studies is that there is no normalization of fascicle length to sarcomere length so it is conceivable that a CP muscle and control muscle could have exactly the same fascicle lengths, yet have different numbers of sarcomeres in series and correspondingly different functional mechanical properties. This would be invisible to the ultrasound method. Direct measurement of intraoperative sarcomere length revealed that sarcomere lengths are indeed longer in CP muscle, suggesting increased passive stiffness (Lieber & Friden, 2002; Ponten *et al.* 2007).

Another proposed mechanism for increased passive stiffness in contractured muscle involves alteration of the tissue itself. Previous studies demonstrated that individual fibres from contractured muscles are stiffer than controls, indicating an alteration within the muscle cell (Friden & Lieber, 2003). This increased stiffness from within the fibre was hypothesized to arise from titin, considered the major passive load-bearing protein within the muscle fibre (Prado *et al.* 2005). Further studies confounded this result showing that bundles of fibres, which include extracellular matrix (ECM), from contractured muscles were more compliant compared to controls, and thus unable to explain the increased stiffness on the whole muscle scale (Lieber *et al.* 2003). A drawback of our previous mechanical studies is that they studied a variety of human muscles, and we have since shown that healthy human muscles have different passive mechanical properties (Ward *et al.* 2009*b*) as was shown for rabbit muscle (Prado *et al.* 2005).

To avoid complications that arise when making comparisons across different muscles, we have taken advantage of the fact that children who are undergoing

Table 1. Patient parameters

Group	*N*	Age	Sex	GMFCS	Popliteal angle	Pass Mech N	SL	OH-Pro	MyHC	Titin
Control	19	15.8 ± 1.8	8 M 11 F	N/A	N/A	14	N/A	12	6	6
CP	33	9.6 ± 4.2	23 M 10 F	I(2),II(13),III(2), IV(6),V(10)	114 ± 15	17	11	12	6	6

Patient parameters for the control and CP groups; control patients do not have Gross Motor Function Classification System (GMFCS; Palisano *et al.* 1997) or popliteal angle measurements. The right columns are the number of subjects whose biopsies were used in the various analysis; many biopsies were used for multiple analysis: passive mechanics sample size (Pass Mech N), *in vivo* sarcomere length (SL), hydroxyproline (OH-pro), myosin heavy chain biopsy analysis (MyHC) and titin biopsy analysis (Titin).

anterior cruciate ligament (ACL) reconstruction with a hamstring autograft have muscle trimmed from the tendon graft that can be harvested and directly compared to the same hamstring muscles from children with CP undergoing surgery. We hypothesized that the passive mechanical properties of spastic muscle are altered in CP and that this could arise across the levels of: protein (titin), cellular (fibre), tissue (fibre bundle including ECM), and/or architecture (sarcomere length). This work will provide further insight into the debilitating mechanism of muscle contracture and drive research on targeted therapies to treat contractures.

Methods

Muscle biopsy collection

Ethical approval for this study conformed to the standards of the *Declaration of Helsinki* and was approved by the Institutional Review Board of the University of California, San Diego Human Research Protection Program. After obtaining consent from parents and age-appropriate assent from children, subjects with CP ($n = 33$) were recruited for this study because they were undergoing hamstring lengthening surgery that involved gracilis and semitendinosus muscles. Control children ($n = 19$) with no history of neurological disorder were recruited because they were undergoing ACL reconstructive surgery with a hamstring autograft using gracilis and semitendinosus tendons that were excised along with a portion of muscle that could be obtained as it was trimmed from the tendon. All patients with CP had developed a contracture requiring surgery, despite receiving conservative treatment. Patients were classified based on clinical measures of the Gross Motor Function Classification System (Palisano *et al.* 1997), popliteal angle, limbs affected and treatment measures of previous surgical lengthening or botulinum toxin injection (Table 1). Muscle biopsies were obtained and either snap frozen in isopentane chilled by liquid nitrogen (−159°C), and stored at −80°C, or placed in glycerinated muscle relaxing solution and stored at −20°C.

In vivo sarcomere lengths

Custom muscle biopsy clamps, modified for pediatric use with 0.5 cm jaw spacing were used to determine *in vivo* sarcomere length (Fig. 1). We previously validated this method against intraoperative laser diffraction (Ward *et al.* 2009*a*). After skin incision and prior to lengthening, gracilis and semitendinosus were identified. A small segment of each muscle was atraumatically isolated by blunt dissection. The custom clamp was then slipped over the bundle, with care to prevent undue tension on the muscle. The child's leg was positioned with 90 deg of hip flexion and 90 deg of knee flexion, and neutral hip abduction–adduction, the clamp was engaged, and the section of muscle within the jaws of the clamp was re-sected and immediately placed in Formalin to fix the biopsy specimen in its *in vivo* configuration. After 2 days of fixation, muscle bundles were isolated on glass slides and sarcomere length was measured by laser diffraction (see below). For control patients receiving ACL reconstruction, hamstring muscles are not accessible in their *in vivo* position, which precludes the use of the biopsy clamps to obtain control values. Thus, for estimation of control sarcomere lengths, we extracted these values from our previous musculoskeletal model (Arnold *et al.* 2010).

Muscle mechanical testing

Biopsies for mechanics were stored in a glycerinated relaxing solution overnight, composed of (mM): potassium propionate (170.0), K_3EGTA (5.0), $MgCl_2$ (5.3), imidazole (10.0), Na_2ATP (21.2), NaN_3 (1.0), glutathione (2.5), 50 μM leupeptin, and 50% (v/v) glycerol. For dissection of fibre or fibre bundle samples, muscles were removed from storage solution and transferred to a relaxing solution at pCa 8.0 and pH 7.1 consisting of (mM): imidazole (59.4), KCH_4O_3S (86.0), $Ca(KCH_4O_3S)_2$ (0.13), $Mg(KCH_4O_3S)_2$ (10.8), K_3EGTA (5.5), KH_2PO_4 (1.0), Na_2ATP (5.1), and 50.0 μM leupeptin. Single fibre segments (1.5–3 mm in length) were carefully dissected and mounted in a chamber in a custom apparatus at room temperature (20°C). Fibres were secured using 10-0 monofilament nylon suture on

one end to a force transducer (Model 405A, sensitivity 10 V g^{-1}, Aurora Scientific, Ontario, Canada) and on the other end to a titanium wire rigidly attached to a rotational bearing (Newport MT-RS; Irvine, CA, USA; Supplementary Fig. S1). Segments displaying obvious abnormalities or discoloration were not used. The sample was transillumated by a 7 mW He–Ne laser to permit sarcomere length measurement by laser diffraction (Lieber *et al.* 1984). Resolution of this method is approximately 5 nm (Baskin *et al.* 1979). The system was calibrated with a 2.50 μm plastic blazed diffraction grating prior to experimentation (Diffraction Gratings, Inc., Nashville, TN, USA).

The fibre was brought to slack length, defined when passive tension was just measurable above the noise level of the force transducer. Sample dimensions were measured optically with a cross-hair reticule mounted on a dissecting microscope and micromanipulators on an *x*–*y* mobile stage. The fibre was then loaded with strains of approximately 0.25 μm sarcomere^{-1} at 100 fibre lengths s^{-1}. Each stretch was held for 2 or 3 min during which stress relaxation was measured, before a sequential stretch was made. Fibres were stretched in total to approximately 100% strain and were saved for titin analysis after mechanical testing. Force data were converted to stress by dividing force by the baseline cross-sectional area value determined assuming a cylindrical sample with an average diameter determined from three separate points along the fibre. Samples were discarded if they did not produce a clear diffraction pattern, if any irregularities appeared along their length during testing, or if they were severed or slipped at either suture attachment point during the test. Muscle bundles were mechanically tested in the same manner as fibres and consisted of approximately 20 fibres and their constitutive ECM.

Mechanical data analysis

All analysis was performed using Matlab (Mathworks Inc., Natick, MA, USA). Relaxed stress after 2 or 3 min was used to fit a relaxed stress *vs.* sarcomere length curve. This curve was fitted with a line for fibres, but with a quadratic for bundles, as there was notable non-linearity in bundle data. For sample fits, sarcomere lengths below slack length are assigned a stress of 0. This produces a 'toe region' due to averaging of the fits across the range of slack sarcomere lengths tested in fibres, generally below 2.5 μm sarcomere length. Only the data beyond the toe region in which most fibres are generating tension are depicted (Fig. 2*A* and *C*). Tangent modulus was calculated at given sarcomere length by taking the derivative of the relaxed stress *vs.* sarcomere length fit at that length. Comparisons of tangent

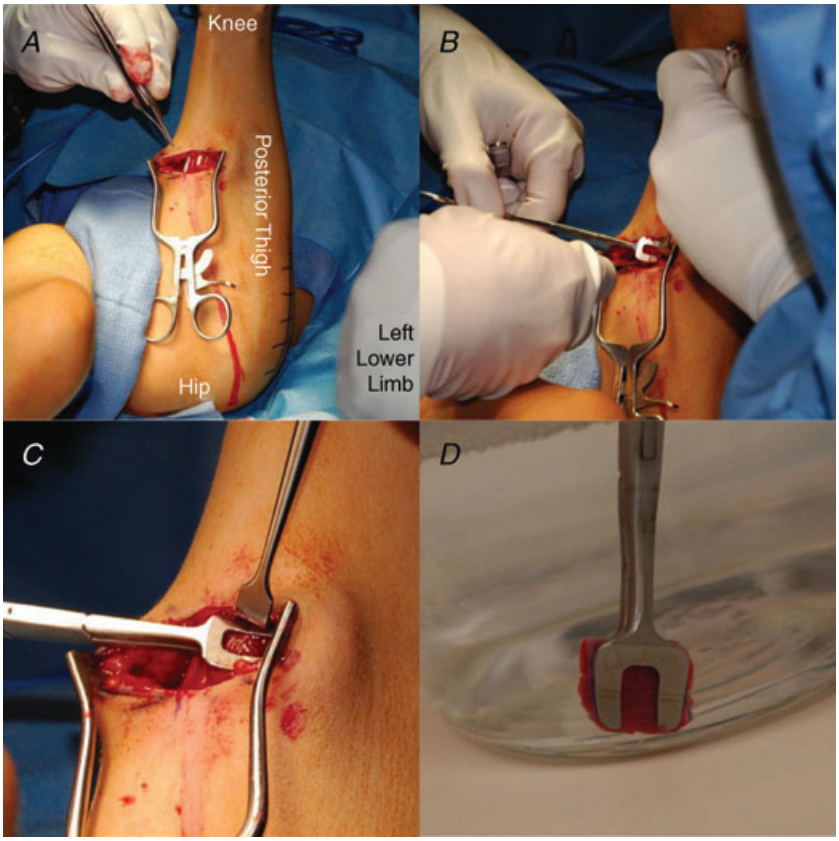

Figure 1. Images of biopsy collection method using clamps for *in vivo* sarcomere length determination
A, hamstring muscle is exposed. *B*, clamp is secured around gracilis muscle with joint position at 90 deg of hip and knee flexion. *C*, close-up view of muscle clamps around the biopsy tissue. *D*, biopsy is dissected from muscle while clamped and fixed in Formalin for subsequent sarcomere length measurement.

stiffness were conducted with a three-way ANOVA for pathology (CP *vs.* control), muscle (gracilis *vs.* semitendinosus; repeated measure), and scale (fibre *vs.* bundle; repeated measure) with results considered significant at $P < 0.05$. All data are presented in the text as mean ± SEM unless otherwise noted.

Protein gels

Titin isoform and MyHC content were analysed on gels from both single fibres after mechanical experiments and from sections of biopsies. Single fibres were stored at −80°C until analysed and boiled for 2 min in 10 μl sodium dodecyl sulfate-vertical agarose gel electrophoresis (SDS-VAGE) sample buffer (comprised of 8 M urea, 2 M thiourea, 3% SDS w/v, 75 mM dithiothreitol (DTT), 0.03% bromophenol blue and 0.05 M Tris-Cl, pH 6.8; Warren *et al.* 2003). For biopsies, a myofibril-rich fraction (~10 mg wet weight) of individual biopsies ($n = 24$ biopsies from 12 patients for titin and MyHC) was homogenized in sample buffer using the Bullet Blender (Next Advance, Inc., Averill Park, NY, USA).

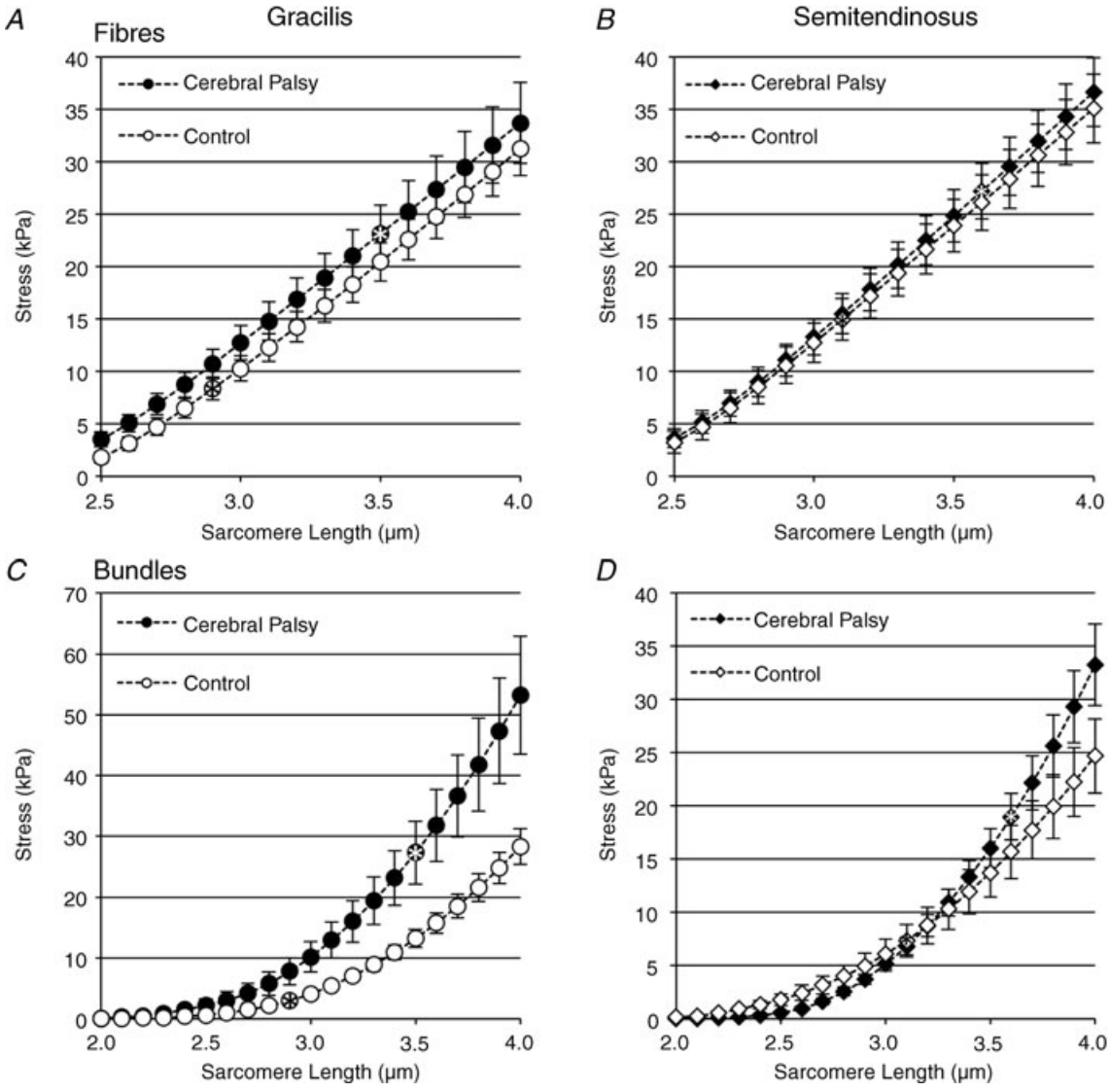

Figure 2. Passive tension as a function of sarcomere length for fibres and bundles, after stress relaxation
Plots represent the average of the fits from each individual sample ± SEM. The stress *vs.* sarcomere length fit was linear for fibres with a R^2 value of 0.962 ± 0.003 (*A* and *B*) and quadratic for bundles with a R^2 value of 0.985 ± 0.002 (*C* and *D*). *A*, gracilis fibres show no difference between CP and control. *B*, semitendinosus fibres show no difference between CP and control. *C*, CP gracilis bundles show a significant increase in stress at high sarcomere lengths compared to control. *D*, CP semitendinosus bundles show a significant increase in stress at high sarcomere lengths compared to control.* inside symbol designates the approximate sarcomere length at 90 deg of hip and knee flexion.

To quantify titin isoforms, the molecular mass of titin in muscle samples was determined using SDS-VAGE. An acrylamide plug was placed at the bottom of the gel to hold the agarose in place. The final composition of this plug was 12.8% acrylamide, 10% v/v glycerol, 0.5 M Tris-Cl, 2.34% *N*,*N*′-diallyltartardiamide, 0.028% ammonium persulfate and 0.152% tetramethylethylenediamine (TEMED). The composition of the agarose gel was 1% w/v SeaKem Gold agarose (Lonza, Basel, Switzerland), 30% v/v glycerol, 50 mM Tris-base, 0.384 M glycine and 0.1% w/v sodium dodecyl sulfate (SDS). Titin standards were obtained from human cadaver soleus (3700 kDa) and rat cardiac muscle (2992 kDa). The standard titin molecular masses are based on sequence analysis of the 300 kb titin gene with a coding sequence contained within 363 exons (Labeit & Kolmerer, 1995; Freiburg *et al.* 2000). These tissues were also homogenized and stored at −80°C until analysis. Before loading onto the gel, a titin standard 'cocktail' was created with the following ratio: 1 unit of human soleus standard:3 units rat cardiac standard:6 units sample buffer. Sample wells were then loaded with both biopsy and rat cardiac homogenate. Human soleus and rat cardiac titin homogenates were loaded into standard lanes. This enabled titin quantification on each gel as previously described (Warren *et al.* 2003). Gels were run at 4°C for 5 h at 15 mA constant current.

To quantify MyHC isoform distribution, homogenized protein solution was resuspended to 0.125 μg μl^{-1} protein (BCA protein assay, Pierce, Rockford, IL, USA) in a sample buffer consisting of DTT (100 mmol l^{-1}), SDS (2%), Tris-base (80 mmol l^{-1}) pH 6.8, glycerol (10%) and bromophenol blue (0.01% w/v). Samples were boiled (2 min) and stored at −80°C. Before loading onto the gel, protein was further diluted 1:15 (0.008 μg μl^{-1}) in the same sample buffer to account for the approximately 50-fold greater sensitivity of the silver stain. Ten microlitres of each sample were loaded in each lane. Total acrylamide concentration was 4% and 8% in the stacking and resolving gels, respectively (bisacrylamide, 1:50). Gels (16 cm × 22 cm, 0.75 mm thick) were run at a constant current of 10 mA for 1 h, and thereafter at constant voltage of 275 V for 22 h at 4–6°C. Gels were silver stained (BioRad, Hercules, CA, USA). MyHC bands were identified and quantified with densitometry (GS-800, BioRad). The progression of the band was compared and identified based on its relative molecular weight to that of a human protein standard prepared (as described above) from a normal semitendinosus biopsy that showed all three human MHC bands (IIa, IIx and I).

Hydroxyproline content

Collagen percentage was determined using a colourimetric analysis of hydroxyproline content. Briefly, muscle samples were hydrolysed in 6 N HCl for 18 h, neutralized, and samples were treated with a chloramine T solution for 20 min at room temperature followed by a solution of *p*-diaminobenzaldehyde for 30 min at 60°C. Sample absorbance was read at 550 nm in triplicate and compared to a standard curve to determine the hydroxyproline content. Hydroxyproline content was converted to collagen using a constant (7.46) that defines the number of hydroxyproline residues in a molecule of collagen.

Immunohistochemistry

Biopsies previously snap-frozen in isopentane were used for immunohistochemistry. Cross-sections (10 μm thick) taken from the midportion of the tissue block were cut on a cryostat at −25°C (Microm HM500, Walldorf, Germany). Serial sections were stained with haematoxylin–eosin to observe general tissue morphology. To investigate ECM components sections were labelled with primary antibodies to fibrillar collagen type I (rabbit polyclonal, Rockland, Gilbertsville, PA, USA) and laminin (rabbit polyclonal, Sigma, St Louis, MI, USA). The secondary antibody used for visualization was an Alexa Fluor 594 goat anti-rabbit immunoglobulin G (Invitrogen, Carlsbad, CA, USA).

Fibre cross-sectional areas were measured from laminin-stained slides using a custom-written macro in ImageJ (NIH, Bethesda, MD, USA). Filtering criteria were applied to insure measurement of actual muscle fibres. These criteria rejected regions with areas below 50 μm^2 or above 5600 μm^2 to eliminate neurovascular structures and 'optically fused' fibres, respectively. Fibres touching the edge of the field were excluded as they were assumed to be incomplete. Regions with circularity below 0.30 or above 1.0 were excluded to prevent inclusion of fibres that were obliquely sectioned.

Results

Passive mechanics

Passive mechanical properties were determined for three fibres per muscle and two muscles per subject, for both control children ($n = 14$) and children with CP ($n = 17$). Fibre diameter was smaller for CP (66.3 ± 2.6 μm) than for control (80.2 ± 2.6 μm; $P < 0.001$) as previously described (Fridén & Lieber, 2003). Slack sarcomere length for control (2.31 ± 0.04 μm) fibres was not significantly different from CP (2.31 ± 0.04 μm (SD); $P > 0.9$) fibres. The stiffness of CP fibres was not significantly different from control for gracilis (control 21.5 ± 1.8 kPa μm^{-1}; CP 21.5 ± 2.4 kPa μm^{-1}; Figs 2*A* and 3*A*) or semitendinosus

(control 22.4 ± 1.8 kPa μm^{-1}; CP 23.6 ± 1.7 kPa μm^{-1}; Figs 2*B* and 3*A*), nor was it significantly different between muscles.

Passive mechanical properties were determined for three bundles on the same biopsy as for fibres. Fibre bundle diameters were not significantly different between control (366.1 ± 15.0 μm) and CP (354.9 ± 15.2 μm; $P > 0.4$) bundles, nor were slack sarcomere lengths (control: 2.27 ± 0.03 μm; CP 2.29 ± 0.03 μm; $P > 0.5$). CP bundles had higher stresses at longer sarcomere lengths for both gracilis and semitendinosus muscle. When comparing the tangent stiffness at 4.0 μm the stiffness of CP bundles was significantly greater than control ($P < 0.05$) for both gracilis (control 36.1 ± 3.9 kPa μm^{-1}; CP 60.4 ± 11.8 kPa μm^{-1}; Figs 2*C* and 3*B*) and semitendinosus (control 25.2 ± 2.9 kPa μm^{-1}; CP 40.7 ± 4.9 kPa μm^{-1}; Figs 2*D* and 3*B*).

The three-way ANOVA with muscle (semitendinosus/gracilis; repeated measure), scale (fibre/bundle; repeated measure) and condition (CP/control) on tangent stiffness revealed a main effect of all three independent measures ($P < 0.05$ for condition and muscle; $P < 0.001$ scale). The results also showed a significant interaction between muscle and scale ($P < 0.05$), with *post hoc* tests revealing gracilis bundles are stiffer than semitendinosus, and a significant interaction of condition and scale, with *post hoc* tests revealing an effect of CP only at the bundle level for semitendinosus ($P < 0.05$).

To determine whether the mechanical changes were related to the clinical observations made on the patients, stiffness was correlated with clinical severity score. There was no significant correlation between stiffness and either Gross Motor Function Classification System or popliteal angle at either the fibre or bundle level (Supplemental Fig. 2*A*). To determine consistency within patients, a correlation was run between gracilis and semitendinosus stiffness within the same patient, or fibre stiffness to bundle stiffness within the same biopsy, but again there were no significant correlations (Supplemental Fig. 2*B* and *C*). There was also a concern that there might be an age effect since the control subjects were slightly older than CP subjects (Table 1) but no significant correlation was found, validating the comparison of control to CP subjects with different ages (Supplemental Fig. 2*D*). Further, the mechanics were compared from patients who underwent a previous hamstring lengthening surgery or botulinum toxin injection prior to biopsy as these may affect stiffness. No significant difference was observed for prior botulinum toxin injection for bundles ($P > 0.3$) or fibres ($P > 0.8$). Only one patient with mechanics measured had undergone a previous lengthening surgery, which was not an outlier among any mechanical measure.

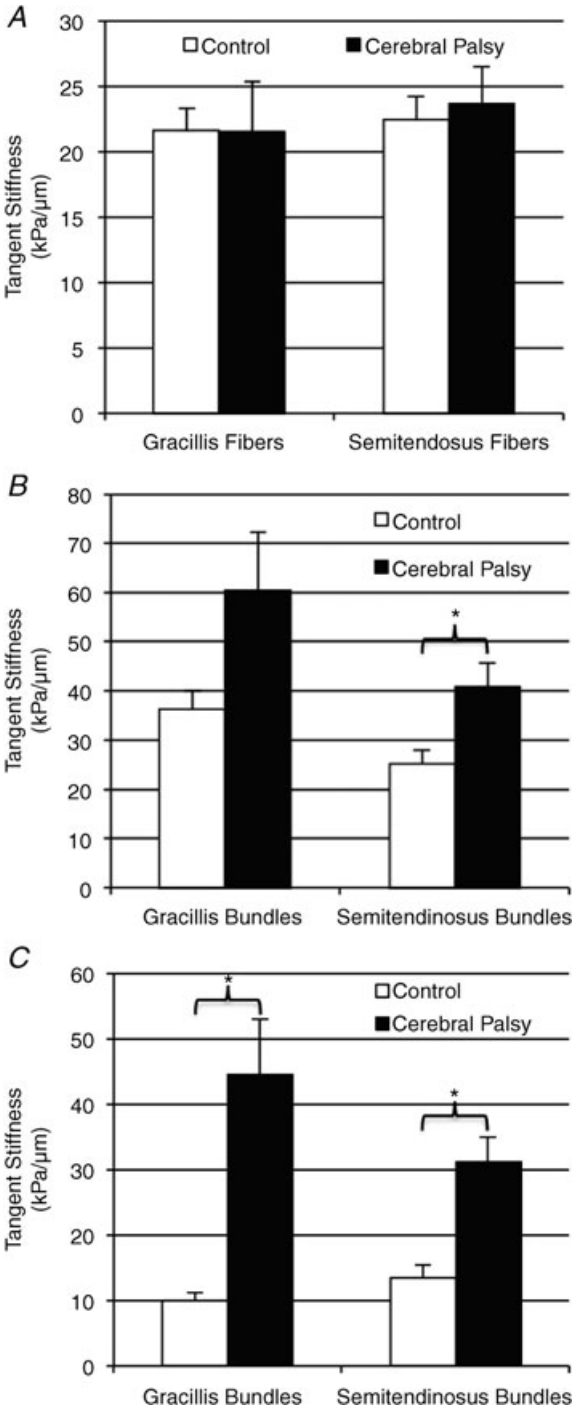

Figure 3. Tangent stiffness of fibres and bundles
Samples are represented with either a linear fit for fibres or a quadratic fit for bundles. *A*, tangent stiffness values at 4.0 μm for single fibres are not changed with CP for either gracilis or semitendinosus muscles. *B*, tangent stiffness values at 4.0 μm for fibre bundles are significantly greater in CP compared to control bundles in both gracilis and semitendinosus ($P < 0.05$). *C*, tangent stiffness values at measured average *in vivo* sarcomere length for CP bundles or the predicted *in vivo* sarcomere length for control bundles show highly elevated values in CP for a joint configuration of 90 deg hip and knee flexion.

In vivo sarcomere lengths

In vivo sarcomere length from cerebral palsy patients of contractured hamstring muscles ($n = 22$) was $3.54 \pm .14\ \mu$m for gracilis and $3.62 \pm .13\ \mu$m for semitendinosus at 90 deg of hip and knee flexion. For control comparison, model results were used as described in Methods (Arnold *et al.* 2010). Both gracilis and semitendinosus had significantly longer sarcomere lengths at 90 deg of hip and knee flexion than predicted by the model by about $0.5\ \mu$m (Fig. 4*A*, $P < 0.05$ for semitendinosus and gracilis). Combining the sarcomere length values with passive mechanical properties demonstrates that CP muscle tissue at these joint angles bears a higher passive load compared to control muscle (Fig. 3*C*).

To determine whether the sarcomere length was associated with functional changes, clinical measures were correlated to sarcomere length. There was a significant correlation between *in vivo* sarcomere length and both Gross Motor Function Classification System ($P < 0.05$) and sarcomere length ($P < 0.05$), indicating that more severely involved patients had longer *in vivo* sarcomere lengths (Fig. 4*B*). There was also a significant negative correlation between popliteal angle and *in vivo* sarcomere length indicating that longer sarcomere lengths were present in joints with more severe contractures (Fig. 4*C*). Together these correlations provide further evidence that *in vivo* sarcomere lengths are elevated in CP.

To compare predicted *in vivo* stiffness of CP muscles compared to control we also evaluated the tangent stiffness at the average *in vivo* sarcomere length of 90 deg of hip and knee flexion for each muscle and condition from the data above. Combining the *in vivo* sarcomere lengths with the mechanical data shows that *in vivo* stiffness is predicted to be much larger for CP muscle (Fig. 3*C*). As fibres had linear stress–strain relationships, the tangent stiffness does not vary with sarcomere length and is thus the same result as the tangent stiffness at $4.0\ \mu$m.

Titin isoforms

To determine if titin size was related to overall muscle stiffness we measured titin molecular mass from a biopsy. The results of a two-way ANOVA showed no significant difference ($P > 0.05$) for CP with mean values of gracilis (control 3588 ± 18 kDa; CP 3667 ± 22 kDa) and semitendinosus (control 3625 ± 19 kDa; CP 3658 ± 26 kDa; Fig. 5) among the samples measured ($n = 24$, 6 per muscle condition). The mass of CP titin was actually larger than that of control suggesting, if anything, a more compliant isoform and unable to account for any increased passive stiffness of the muscle as a whole.

The effect of titin isoform was also investigated on single fibres that had previously undergone passive mechanical testing. A two-way ANOVA showed no significant difference ($P > 0.1$) between titin isoform sizes for gracilis (control 3758 ± 24 kDa; CP 3772 ± 36 kDa) or semitendinosus (control 3729 ± 40 kDa; CP 3797 ± 40 kDa) among the single fibres measured ($n = 55$). CP fibres having equivalent titin isoform size to control fibres is consistent with the fact that CP and control fibres have equivalent stiffness. The effect of titin isoform size on the variability in mechanical stiffness of fibres was also investigated, but there was not a significant correlation between titin size and fibre stiffness within single fibres

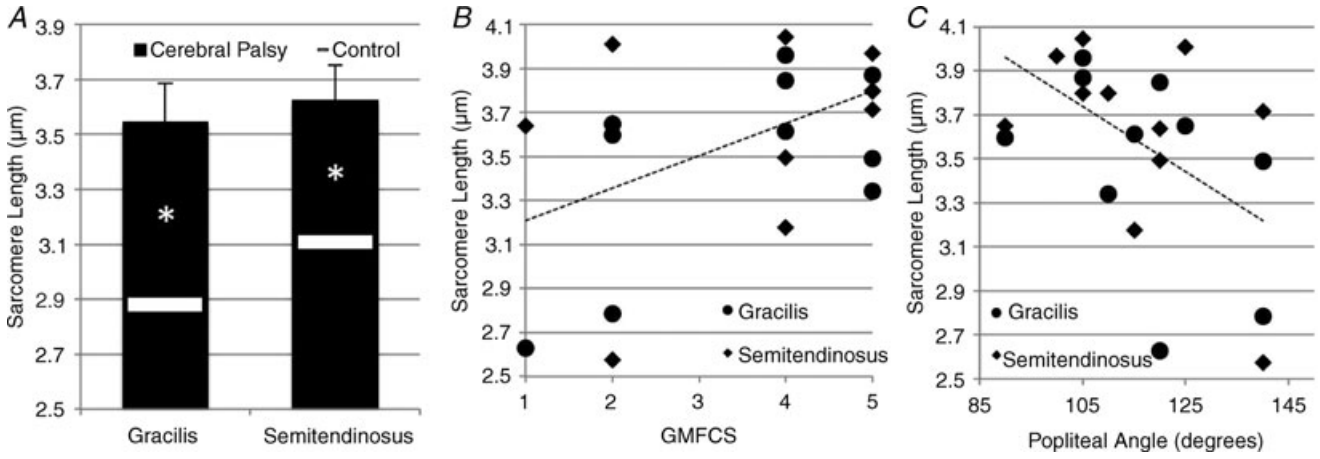

Figure 4. *In vivo* sarcomere length of gracilis and semitendinosus
A, measured *in vivo* sarcomere length with 90 deg of hip and knee flexion ± SEM for CP subjects in gracilis and semitindenosus ($P < 0.05$). Solid white line represents predicted sarcomere length for control children. *B*, correlation between *in vivo* sarcomere length measured for CP subjects and their Gross Motor Function Classification System (GMFCS) shows a positive significant correlation ($P < 0.05$), meaning subjects with longer *in vivo* sarcomeres are more severely affected patients. *C*, correlation between *in vivo* sarcomere length and popliteal angle is negative and significant ($P < 0.05$), meaning subjects with less knee extension have longer sarcomere lengths.

(Supplemental Fig. S3). The molecular masses are larger for single fibres than for the whole biopsies, possibly due to modified preparation methods.

Collagen content

Collagen content of the biopsies was measured ($n = 40$, 10 per muscle per condition) as collagen is thought to be the primary load-bearing structure of the ECM within muscle (Purslow, 1989). CP muscles had significantly higher collagen concentrations in both gracilis (control $8.0 \pm 1.6\,\mu g\,(mg\ wet\ weight)^{-1}$); CP $11.2 \pm 2.6\,\mu g\,(mg\ wet\ weight)^{-1}$) and semitendinosus (control $4.0 \pm 0.3\,\mu g\,(mg\ wet\ weight)^{-1}$); CP $8.8 \pm 0.8\,\mu g\,(mg\ wet\ weight)^{-1}$) as determined by a two-way ANOVA on muscle and condition (Fig. 6, $P < 0.05$). Collagen content was elevated in both gracilis and semitendinosus, although *post hoc* tests revealed a significant difference only in semitendinosus ($P < 0.001$). Gracilis also tended to have higher collagen concentrations corresponding to the relationship seen in passive bundle stiffness. The collagen content was not significantly different for patients who underwent a previous lengthening surgery ($P > 0.5$) or botulinum toxin injections ($P > 0.8$) prior to biopsy.

Collagen was also visualized by immunohistochemistry. Qualitative results show an increase in fibrillar collagen type I (Fig. 7*A–D*) in muscle from children with CP, corresponding the hydroxyproline results. There was no apparent mislocalization of collagen; however, an increased frequency of large collagen deposits was observed. Laminin, a component of the basal lamina, also showed marked increase in CP muscle (Fig. 7*E–H*). These results demonstrate an increase of ECM material that includes, but is not limited to collagen. While histological evidence shows an increase in ECM material in muscle from children with cerebral palsy, there is also a corresponding decrease in fibre cross-sectional area (from $3141 \pm 375\,\mu m^2$ for controls to $1255 \pm 226\,\mu m^2$; $P < 0.001$ for cerebral palsy) as has been previously reported (Fridén & Lieber, 2003).

Myosin heavy chain

To determine whether any of the single mechanical fibre data might be confounded by systematic differences in muscle fibre type between patient populations, myosin heavy chain isoform content was measured ($n = 35$ fibres). One-way ANOVA comparing tangent stiffness of different fibre types did not produce a significant result for either CP or control fibres ($P > 0.05$; Supplemental Fig. S4).

To determine the distribution of different fibre types for hamstring muscles in CP myosin heavy chain content was measured from a sample of biopsies ($n = 24$, 6 per muscle per condition). CP muscles had increased slow myosin heavy chain expression (gracilis – control $29.3 \pm 1.9\%$ to CP $40.0 \pm 2.5\%$; semitendinosus – control $29.7 \pm 1.7\%$ to CP $41.0 \pm 3.3\%$; $P < 0.001$; Fig. 8), but there was no significant change in either of the fast isoforms measured (IIa or IIx). Since myosin heavy chain is the primary determinant of fibre type, these results demonstrate a shift to slower fibres in CP muscle. There was no significant difference between gracilis and semitendinosus muscles.

Discussion

The most significant finding of this study is that muscle tissue from children with CP is significantly stiffer compared to typically developing children. This increased

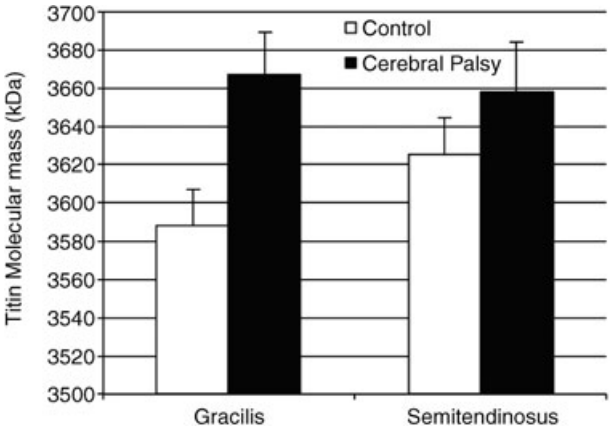

Figure 5. Molecular mass of titin isoforms of CP and control subjects in gracilis and semitendinosus muscles
Two-way ANOVA shows no significant effect of pathology on molecular mass ($P > 0.05$). Although not significant, the trend for molecular mass of titin in CP muscles is larger than control suggesting, if anything, more compliant fibres due to titin alterations.

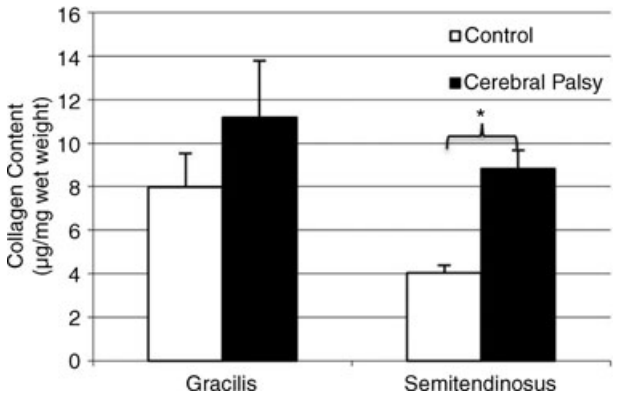

Figure 6. Collagen content of muscle biopsies shows significantly higher collagen content in CP biopsies
The results of this assay are consistent with the increased stiffness observed in fibre bundles (Fig. 4). *indicates a significant post hoc difference between control and CP for the semintendinosus ($p < 001$).

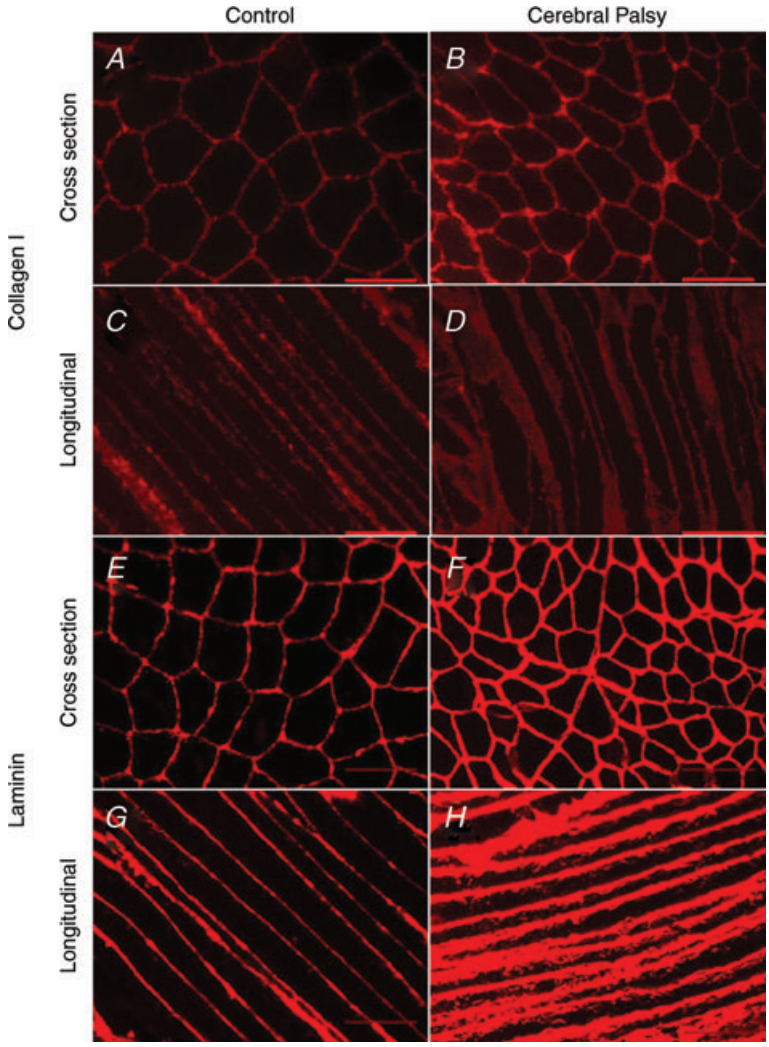

Figure 7. Immunohistochemistry of muscle biopsies show qualitatively increased levels of ECM in CP (*B*, *D*, *F* and *H*) compared to control (*A*, *C*, *E* and *G*) children
Representative images with primary antibody to fibrillar collagen type I in cross section (*A* and *B*) and longitudinal section (*C* and *D*). Representative images with primary antibody to laminin of the basal lamina, in cross section (*E* and *F*) and longitudinal section (*G* and *H*). Note that muscle fibers from children with CP are slightly smaller with a great amount of Collagen I and laminin, two of the major components of the extracellular matrix. Scale bars represent 100 μm.

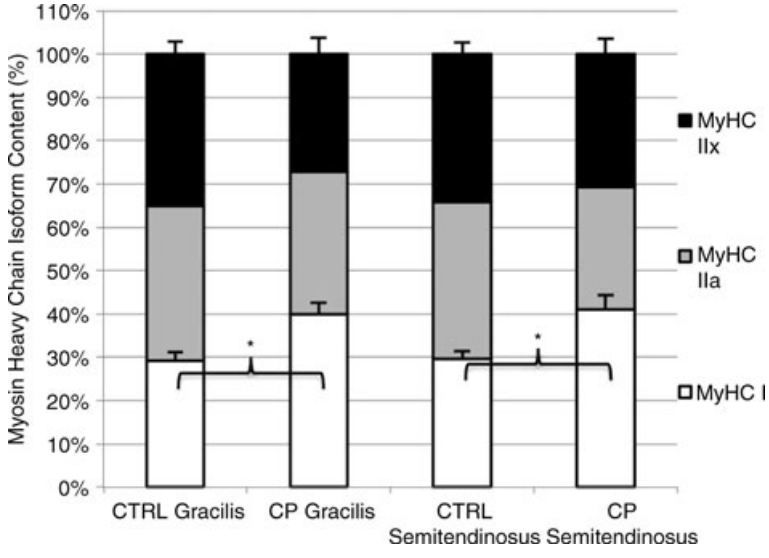

Figure 8. Myosin heavy chain isoforms
There was a significant increase in myosin heavy chain I in CP muscles compared to control suggesting contractured fibres have a slower phenotype. There was no significant difference between muscles. *represents significant difference in MyHC 1 percentage between control and CP muscles ($p < 0.001$)

passive stiffness is accompanied by an increase in collagen content and is made even more functionally significant in that *in vivo* sarcomere length of CP hamstring muscles is significantly longer compared to predictions for control children. Taken together, these data provide a mechanistic explanation for the increased joint and muscle stiffness observed in these contracture patients. While fibre bundles were different between CP and control muscle, we found no significant difference in mechanical properties at the single fibre level of muscle and no change in titin isoform size. Thus, we conclude that, for human hamstring muscles, increased passive tension in contracture is due to a change in ECM stiffness and increased *in vivo* functional sarcomere length rather than any intracellular alteration.

Bundle mechanics

While fibres contribute to passive tension of muscle, muscle ECM plays an important role in passive mechanics, especially at longer sarcomere lengths. The results show a significant increase in the tangent stiffness of fibre bundles from CP patients. While fibres were fitted well with a linear stress–sarcomere length relationship, fibre bundles required a non-linear quadratic fit. This non-linearity results in similar tissue stiffness at small strains, but significantly increased stiffness at long sarcomere lengths of the CP muscle tissue. Muscle contractures often limit joint range of motion suggesting that there are large *in vivo* strains on the muscle. We thus believe that, *in vivo*, the ECM bears a large portion of the passive muscle load.

Collagen is considered the primary load-bearing structure within muscle ECM (Purslow, 1989). We hypothesized that an increase in collagen content of CP muscle could lead to the increased passive stiffness seen in bundles. Using a hydroxyproline assay to test the hypothesis, the results demonstrate a significant increase in collagen within CP muscle. Although these data are presented in micrograms of collagen per milligram of muscle wet weight, they are similar to previous data presenting collagen as a percent of dry weight (Bendall, 1967), using the assumption that muscle is approximately 80% water (Ward & Lieber, 2005). Increased collagen was also observed by immunohistochemistry along with another ECM component, laminin, a critical component for cellular attachment to the basal lamina. These results are in agreement with a previous study showing increased collagen content within CP muscle (Booth *et al.* 2001). Many additional factors may be playing a role in the increased ECM stiffness. The organization of collagen, the distribution of collagen types, or the proteoglycan content all could be altered in CP to create a stiffer ECM and represent areas of further investigation. Immunohistochemistry of other muscle proteins (α-actinin, desmin, dystrophin) revealed no obvious differences between patient groups.

One previous study investigated the mechanics of fibre bundles from contractured muscle tissue (Lieber *et al.* 2003). Despite finding stiffer fibres we found more compliant bundles in CP muscle. This result is difficult to reconcile with the increased passive stiffness of the whole muscle that has been reported. The previous study was conducted on biopsies taken from various muscles that were not matched between populations, which could account for some of these differences and all muscles were from upper extremities, which may respond differently to spasticity. In addition, the ECM from upper extremity muscles was highly deranged in the contractured muscles (see Fig. 2 of Lieber *et al.* 2003) making area fraction measurements from these specimens difficult. It is possible that the area fraction of ECM was overestimated, resulting in artificially low values for bundle modulus. Finally, the non-linear behaviour of upper extremity muscles was quantified by only fitting data to the linear portion of the sarcomere length–stress curve. The current method represents a more accurate method for handling analysis of the non-linear relationships.

Sarcomere organization

Sarcomere length operating ranges of semitendinosus and gracilis muscles are unknown, although muscles are typically believed to operate on the plateau of the length–tension curve (2.5–2.7 μm for human skeletal muscle; Walker & Schrodt, 1974). A previous study demonstrated that spastic muscle operates at longer sarcomere lengths than control (Lieber & Fridén, 2002), which would lead to a larger observed passive stiffness such as that seen in contracture. We measured *in vivo* sarcomere lengths of patients with CP at a defined joint angle and compared these values to sarcomere lengths of control subjects that were calculated based on *in vivo* sarcomere lengths, moment arms and muscle–tendon lengths (Arnold *et al.* 2010). The results showed that the CP sarcomere lengths are significantly longer than those predicted from the model. The lengths measured were also much longer than optimal sarcomere length, lending further evidence to the idea that they are overly stretched in contracture. With CP subjects operating at longer lengths of the passive length–tension relationship, this means that the muscle is experiencing higher stresses not only due to material property changes, but also due to this shift along the passive length–tension curve. This difference becomes more pronounced as the knee extends and the hip flexes, and may limit range of motion for children with contractures.

It is often stated that muscle adds or subtracts serial sarcomeres to optimal sarcomere length *in vivo* (Williams

& Goldspink, 1973). Long *in vivo* sarcomeres suggest an inability of the muscle to add sarcomeres in series, which would be exacerbated during growth spurts, which have been associated with the onset of muscle contractures (Janice & Alwyn, 2005). The very long sarcomere lengths observed *in vivo* clearly imply that muscles from children with CP are under high stress. The source of the force that creates or opposes this stress is not known. However, we have speculated, based on analysis of the transcriptome, that muscles from children with CP are unable to grow serially in response to the stretch imposed by osteogenesis (Smith *et al.* 2009). It is also possible that muscles would decrease their serial sarcomere number, which would provide a resistive force since the changes could be slow and accompanied by reinforcement of the muscle fibre by the ECM. Muscle contracture is often described as a 'shortened' muscle; our finding of increased *in vivo* sarcomere length corresponds with the notion that muscle shortening is derived from fewer series sarcomeres, not shortened sarcomeres. Longer *in vivo* sarcomere lengths are an important factor for both passive and active force production of skeletal muscle. Previous research has demonstrated that muscles from children with CP are smaller than those of control children, yet muscle force production is reduced to an even greater extent indicating a dysfunction of active muscle force production in CP (Elder *et al.* 2003; Moreau *et al.* 2010). A consequence of having longer *in vivo* sarcomere lengths for children with CP is the muscle will be working at different portions along its active length–tension curve (Gordon *et al.* 1966) compared to control subjects. Based on measured human filament lengths (Walker & Schrodt, 1974) and the increase in $\sim$0.5 μm sarcomere length, the decrease in force from a typically developing child on the plateau of the length–tension curve to a child with CP on the descending limb would be 33%. It is interesting to note that this is on the same scale as the reduction in force that is not accounted for by decreased muscle size in these patients (Elder *et al.* 2003; Moreau *et al.* 2010). Thus, perhaps altered *in vivo* sarcomere length operating range represents a significant functional alteration in muscles from children CP and demonstrates that these muscles are not simply changing sarcomere number to 're-optimize' the muscle after injury.

Potential mechanisms of contracture formation

It is possible that the changes in ECM and *in vivo* sarcomere length take place simultaneously and independently, or that one precedes and directly affects the other. If these two alterations of CP muscle are not causal, they could be a consequence of the same factors within spastic muscle. Previous research showed that myostatin, a negative regulator of muscle growth, also stimulates proliferation of muscle fibroblasts and the release of ECM proteins (Li *et al.* 2008). Myostatin mRNA has also been shown as significantly increased in CP muscle of the upper extremity (Smith *et al.* 2009). Alternatively, transforming growth factor-β1 has been shown to induce a shift in satellite cells from a myogenic lineage to fibrobasts (Li *et al.* 2004). This process also has the potential to limit growth through satellite cell depletion and increase the ECM secreting cell population.

Longer *in vivo* sarcomeres of CP muscles demonstrate that there is increased sarcomere strain, which has been shown to directly induce skeletal muscle injury (Patel *et al.* 2004). Repeated strain-induced injuries have been shown to drastically increase collagen content and fibrosis in skeletal muscle (Stauber, 2004). The effects of chronic strain injuries persist for months or even years and could be responsible for the effects of muscle in contracture. Repeated strain-induced injury also results in lower force-producing capacity of muscle, which may provide another explanation for the reduced specific tension of CP muscle (Proske & Morgan, 2001). The increased fibrosis and stiffness of muscle contracture could also be a compensatory mechanism to limit further strain-induced injury.

There is also potential for a fibrosis induced from spasticity to lead directly to a limitation of longitudinal growth. Satellite cells responsible for muscle growth rely on migration across the basement membrane during activation with the release of matrix metalloproteases (Chen & Li, 2009). Skeletal muscle fibrosis could impede muscle regeneration by forming a mechanical barrier to this process (Chen & Li, 2009). Stem cell differentiation is also sensitive to the elasticity of the matrix in which it is embedded (Engler *et al.* 2006). Our study demonstrated an altered stiffness of the ECM in contracture tissue that could lead to an inhibition of satellite cell activation or proliferation (Boonen *et al.* 2009; Gilbert *et al.* 2010) and perhaps even predispose muscle stem cells to differentiate toward the fibroblast lineage. It is also possible that fibrosis and lack of growth create a vicious cycle that leads to muscle contracture.

Titin isoforms

Since titin isoform size is related to muscle passive tension (Prado *et al.* 2005), we hypothesized that shorter titin isoforms would be present in muscle contracture leading to increased stiffness. However, our results show no difference in titin size between CP and control muscles. Thus, we conclude that titin is not altered in CP to cause contracture, at least not in a manner that alters size. Titin isoform changes have been reported in cardiac disease (Neagoe *et al.* 2003), but literature on titin isoform changes in skeletal muscle is sparse. A previous study investigating

titin isoform in spastic muscles of stroke patients also found no change in isoform size (Olsson *et al.* 2006).

Fibre mechanics

While titin isoform size contributes to single fibre mechanics, other proteins or organization of fibre material could be responsible for an increased passive tension at the cellular level. Two previous studies did demonstrate stiffer muscle fibres for spastic patients. These studies each had important differences, however. In one the muscle fibres tested were from a range of muscles which was not the same in the spastic and control groups (Friden & Lieber, 2003). This is a confounding issue because it is known that different muscles have different passive mechanical properties (Prado *et al.* 2005). Another showed increased stiffness only in fast fibres with an increase in the proportion of fast fibres (Olsson *et al.* 2006). We did not see a corresponding shift to fast fibres of our muscles, and in fact showed a significant increase in type I myosin heavy chain of CP muscles indicating a shift to slower fibres (Fig. 8). Overall, previous studies have shown disagreement on whether spastic muscles gain a faster or slower phenotype, which could be muscle specific (Brooke & Engel, 1969; Scelsi *et al.* 1984; Jakobsson *et al.* 1991). However, the most straightforward interpretation of our data is that over-activity resulting from spasticity drives a shift to slower fibres. It is also important to note that the previous study was performed with vastus lateralis muscle biopsies (Olsson *et al.* 2006), which show much less spasticity and contracture development compared to the medial hamstrings studied here (Damiano *et al.* 2002; Pierce *et al.* 2008). Future studies across a wider range of muscles are required to ultimately resolve these ambiguities.

Study limitations

One important limitation of this study is the subject heterogeneity. CP is a spectrum disorder and here we have primarily examined only the commonly shared parameters of this range of subjects with spastic CP. A more detailed analysis could be attempted using patient stratification by clinical parameters, Gross Motor Function Classification System, popliteal angle, limbs affected, age and treatment regimens. However, due to limitations of the sample size and the high variability of parameters in working with human subjects, this was not possible. We were able to demonstrate a significant correlation between severity measures and sarcomere length, which helped to mitigate the fact that we are relying on model data for our comparison with *in vivo* sarcomere lengths control children.

The source of controls for this study is not ideal since the patients had sustained an ACL tear. However, these patients were several months removed from the injury and had normal mobility at the time of surgery. Our approach represents the best available source of normal hamstring muscle from a pediatric population. These subject groups were not perfectly age-matched, although they all came from a pediatric population, as ACL surgeries do not occur prior to the teenage years whereas hamstring-lengthening surgeries often occur much earlier. However, our passive mechanical data did not correlate with age, suggesting that these small age discrepancies did not affect our outcomes. The subjects also underwent varied previous treatments, of which previous hamstring-lengthening surgery and botulinum toxin injections into the hamstrings was tracked. These variables were analysed in relation to mechanical measures and collagen content, but no relationship was found. These treatment effects are further complicated by highly variable times since treatment.

Summary

It is known that muscle contractures result from the UMN lesion in CP. Here, using a larger and more controlled study then previous ones, we showed increased passive stiffness of fibre bundles and increased sarcomere length *in vivo*. Together, these properties create a muscle in CP that experiences much higher stresses with increasing muscle length and clearly contributes to the development of muscle and joint contractures. Future studies are required to understand the mechanistic basis for the sarcomere length change and increased ECM content in CP as these clearly represent targets for therapy.

References

Arnold EM, Ward SR, Lieber RL & Delp SL (2010). A model of the lower limb for analysis of human movement. *Ann Biomed Eng* **38**, 269–279.

Bache CE, Selber P & Graham HK (2003). (ii) The management of spastic diplegia. *Current Orthopaedics* **17**, 88–104.

Baskin RJ, Roos KP & Yeh Y (1979). Light diffraction study of single skeletal muscle fibres. *Biophys J* **28**, 45–64.

Beals RK (2001). Treatment of knee contracture in cerebral palsy by hamstring lengthening, posterior capsulotomy, and quadriceps mechanism shortening. *Dev Med Child Neurol* **43**, 802–805.

Bendall JR (1967). The elastin content of various muscles of beef animals. *J Sci Food Agriculture* **18**, 553–558.

Boonen KJ, Rosaria-Chak KY, Baaijens FP, Van Der Schaft DW & Post MJ (2009). Essential environmental cues from the satellite cell niche: optimizing proliferation and differentiation. *Am J Physiol Cell Physiol* **296**, C1338–C1345.

Booth CM, Cortina-Borja MJ & Theologis TN (2001). Collagen accumulation in muscles of children with cerebral palsy and correlation with severity of spasticity. *Dev Med Child Neurol* **43**, 314–320.

Brooke MH & Engel WK (1969). The histographic analysis of human muscle biopsies with regard to fiber types. 2. Diseases of the upper and lower motor neuron. *Neurology* **19**, 378–393.

Chen X & Li Y (2009). Role of matrix metalloproteinases in skeletal muscle: migration, differentiation, regeneration and fibrosis. *Cell Adh Migr* **3**, 337–341.

Conway D & Sakai T (1960). Caffeine contracture. *Proc Natl Acad Sci U S A* **46**, 897–903.

Crenna P (1998). Spasticity and 'spastic' gait in children with cerebral palsy. *Neurosci Biobehav Rev* **22**, 571–578.

Damiano DL, Quinlivan JM, Owen BF, Payne P, Nelson KC & Abel MF (2002). What does the Ashworth scale really measure and are instrumented measures more valid and precise? *Dev Med Child Neurol* **44**, 112–118.

Elder GC, Kirk J, Stewart G, Cook K, Weir D, Marshall A & Leahey L (2003). Contributing factors to muscle weakness in children with cerebral palsy. *Dev Med Child Neurol* **45**, 542–550.

Engler AJ, Sen S, Sweeney HL & Discher DE (2006). Matrix elasticity directs stem cell lineage specification. *Cell* **126**, 677–689.

Farmer SE & James M (2001). Contractures in orthopaedic and neurological conditions: a review of causes and treatment. *Disabil Rehabil* **23**, 549–558.

Fergusson D, Hutton B & Drodge A (2007). The epidemiology of major joint contractures: a systematic review of the literature. *Clin Orthop Relat Res* **456**, 22–29.

Freiburg A, Trombitas K, Hell W, Cazorla O, Fougerousse F, Centner T, Kolmerer B, Witt C, Beckmann JS, Gregorio CC, Granzier H & Labeit S (2000). Series of exon-skipping events in the elastic spring region of titin as the structural basis for myofibrillar elastic diversity. *Circ Res* **86**, 1114–1121.

Friden J & Lieber RL (2003). Spastic muscle cells are shorter and stiffer than normal cells. *Muscle Nerve* **27**, 157–164.

Gilbert PM, Havenstrite KL, Magnusson KE, Sacco A, Leonardi NA, Kraft P, Nguyen NK, Thrun S, Lutolf MP & Blau HM (2010). Substrate elasticity regulates skeletal muscle stem cell self-renewal in culture. *Science* **329**, 1078–1081.

Gordon AM, Huxley AF & Julian FJ (1966). The variation in isometric tension with sarcomere length in vertebrate muscle fibres. *J Physiol* **184**, 170–192.

Hodgkin AL & Horowicz P (1960). Potassium contractures in single muscle fibres. *J Physiol* **153**, 386–403.

Jakobsson F, Edstrom L, Grimby L & Thornell LE (1991). Disuse of anterior tibial muscle during locomotion and increased proportion of type II fibres in hemiplegia. *J Neurol Sci* **105**, 49–56.

Janice MQ & Alwyn A (2005). Musculoskeletal problems in cerebral palsy. *Current Paediatrics* **15**, 9–14.

Kerr Graham H & Selber P (2003). Musculoskeletal aspects of cerebral palsy. *J Bone Joint Surg Br* **85**, 157–166.

Labeit S & Kolmerer B (1995). Titins: giant proteins in charge of muscle ultrastructure and elasticity. *Science* **270**, 293–296.

Li Y, Foster W, Deasy BM, Chan Y, Prisk V, Tang Y, Cummins J & Huard J (2004). Transforming growth factor-beta1 induces the differentiation of myogenic cells into fibrotic cells in injured skeletal muscle: a key event in muscle fibrogenesis. *Am J Pathol* **164**, 1007–1019.

Li ZB, Kollias HD & Wagner KR (2008). Myostatin directly regulates skeletal muscle fibrosis. *J Biol Chem* **283**, 19371–19378.

Lieber RL, Yeh Y & Baskin RJ (1984). Sarcomere length determination using laser diffraction. Effect of beam and fiber diameter. *Biophys J* **45**, 1007–1016.

Lieber RL & Friden J (2002). Spasticity causes a fundamental rearrangement of muscle-joint interaction. *Muscle Nerve* **25**, 265–270.

Lieber RL, Runesson E, Einarsson F & Friden J (2003). Inferior mechanical properties of spastic muscle bundles due to hypertrophic but compromised extracellular matrix material. *Muscle Nerve* **28**, 464–471.

Lorentzen J, Grey MJ, Crone C, Mazevet D, Biering-Sorensen F & Nielsen JB (2010). Distinguishing active from passive components of ankle plantar flexor stiffness in stroke, spinal cord injury and multiple sclerosis. *Clin Neurophysiol* **121**, 1939–1951.

Lukban MB, Rosales RL & Dressler D (2009). Effectiveness of botulinum toxin A for upper and lower limb spasticity in children with cerebral palsy: a summary of evidence. *J Neural Transm* **116**, 319–331.

Malaiya R, McNee AE, Fry NR, Eve LC, Gough M & Shortland AP (2007). The morphology of the medial gastrocnemius in typically developing children and children with spastic hemiplegic cerebral palsy. *J Electromyogr Kinesiol* **17**, 657–663.

Mirbagheri MM, Barbeau H, Ladouceur M & Kearney RE (2001). Intrinsic and reflex stiffness in normal and spastic, spinal cord injured subjects. *Exp Brain Res* **141**, 446–459.

Mohagheghi AA, Khan T, Meadows TH, Giannikas K, Baltzopoulos V & Maganaris CN (2007). Differences in gastrocnemius muscle architecture between the paretic and non-paretic legs in children with hemiplegic cerebral palsy. *Clin Biomech (Bristol, Avon)* **22**, 718–724.

Mohagheghi AA, Khan T, Meadows TH, Giannikas K, Baltzopoulos V & Maganaris CN (2008). *In vivo* gastrocnemius muscle fascicle length in children with and without diplegic cerebral palsy. *Dev Med Child Neurol* **50**, 44–50.

Moreau NG, Simpson KN, Teefey SA & Damiano DL (2010). Muscle architecture predicts maximum strength and is related to activity levels in cerebral palsy. *Phys Ther* **90**, 1619–1630.

Neagoe C, Opitz CA, Makarenko I & Linke WA (2003). Gigantic variety: expression patterns of titin isoforms in striated muscles and consequences for myofibrillar passive stiffness. *J Muscle Res Cell Motil* **24**, 175–189.

O'Dwyer NJ, Ada L & Neilson PD (1996). Spasticity and muscle contracture following stroke. *Brain* **119**, 1737–1749.

Olsson MC, Kruger M, Meyer LH, Ahnlund L, Gransberg L, Linke WA & Larsson L (2006). Fibre type-specific increase in passive muscle tension in spinal cord-injured subjects with spasticity. *J Physiol* **577**, 339–352.

Palisano R, Rosenbaum P, Walter S, Russell D, Wood E & Galuppi B (1997). Development and reliability of a system to classify gross motor function in children with cerebral palsy. *Dev Med Child Neurol* **39**, 214–223.

Patel TJ, Das R, Friden J, Lutz GJ & Lieber RL (2004). Sarcomere strain and heterogeneity correlate with injury to frog skeletal muscle fiber bundles. *J Appl Physiol* **97**, 1803–1813.

Pierce SR, Barbe MF, Barr AE, Shewokis PA & Lauer RT (2008). Roles of reflex activity and co-contraction during assessments of spasticity of the knee flexor and knee extensor muscles in children with cerebral palsy and different functional levels. *Phys Ther* **88**, 1124–1134.

Ponten E, Gantelius S & Lieber RL (2007). Intraoperative muscle measurements reveal a relationship between contracture formation and muscle remodeling. *Muscle Nerve* **36**, 47–54.

Prado LG, Makarenko I, Andresen C, Kruger M, Opitz CA & Linke WA (2005). Isoform diversity of giant proteins in relation to passive and active contractile properties of rabbit skeletal muscles. *J Gen Physiol* **126**, 461–480.

Proske U & Morgan DL (2001). Muscle damage from eccentric exercise: mechanism, mechanical signs, adaptation and clinical applications. *J Physiol* **537**, 333–345.

Purslow PP (1989). Strain-induced reorientation of an intramuscular connective tissue network: implications for passive muscle elasticity. *J Biomech* **22**, 21–31.

Rose J & McGill KC (2005). Neuromuscular activation and motor-unit firing characteristics in cerebral palsy. *Dev Med Child Neurol* **47**, 329–336.

Rosenbaum P, Paneth N, Leviton A, Goldstein M, Bax M, Damiano D, Dan B & Jacobsson B (2007). A report: the definition and classification of cerebral palsy April 2006. *Dev Med Child Neurol Suppl* **109**, 8–14.

Savage AO & Atanga KG (1988). Caffeine- and potassium-induced contractures of mouse isolated soleus muscle: effects of verapamil, manganese, EGTA and calcium withdrawal. *Clin Exp Pharmacol Physiol* **15**, 901–911.

Scelsi R, Lotta S, Lommi G, Poggi P & Marchetti C (1984). Hemiplegic atrophy. Morphological findings in the anterior tibial muscle of patients with cerebral vascular accidents. *Acta Neuropathol* **62**, 324–331.

Shortland AP, Harris CA, Gough M & Robinson RO (2002). Architecture of the medial gastrocnemius in children with spastic diplegia. *Dev Med Child Neurol* **44**, 158–163.

Sinkjaer T & Magnussen I (1994). Passive, intrinsic and reflex-mediated stiffness in the ankle extensors of hemiparetic patients. *Brain* **117**, 355–363.

Smith LR, Ponten E, Hedstrom Y, Ward SR, Chambers HG, Subramaniam S & Lieber RL (2009). Novel transcriptional profile in wrist muscles from cerebral palsy patients. *BMC Med Genomics* **2**, 44.

Stackhouse SK, Binder-Macleod SA & Lee SC (2005). Voluntary muscle activation, contractile properties, and fatigability in children with and without cerebral palsy. *Muscle Nerve* **31**, 594–601.

Stauber WT (2004). Factors involved in strain-induced injury in skeletal muscles and outcomes of prolonged exposures. *J Electromyogr Kinesiol* **14**, 61–70.

Tilton AH (2006). Therapeutic interventions for tone abnormalities in cerebral palsy. *NeuroRx* **3**, 217–224.

Walker SM & Schrodt GR (1974). I segment lengths and thin filament periods in skeletal muscle fibers of the Rhesus monkey and the human. *Anat Rec* **178**, 63–81.

Ward SR & Lieber RL (2005). Density and hydration of fresh and fixed human skeletal muscle. *J Biomech* **38**, 2317–2320.

Ward SR, Takahashi M, Winters TM, Kwan A & Lieber RL (2009*a*). A novel muscle biopsy clamp yields accurate *in vivo* sarcomere length values. *J Biomech* **42**, 193–196.

Ward SR, Tomiya A, Regev GJ, Thacker BE, Benzl RC, Kim CW & Lieber RL (2009*b*). Passive mechanical properties of the lumbar multifidus muscle support its role as a stabilizer. *J Biomech* **42**, 1384–1389.

Warren CM, Krzesinski PR & Greaser ML (2003). Vertical agarose gel electrophoresis and electroblotting of high-molecular-weight proteins. *Electrophoresis* **24**, 1695–1702.

Wiart L, Darrah J & Kembhavi G (2008). Stretching with children with cerebral palsy: what do we know and where are we going? *Pediatr Phys Ther* **20**, 173–178.

Williams PE & Goldspink G (1973). The effect of immobilization on the longitudinal growth of striated muscle fibres. *J Anat* **116**, 45–55.

Yeargin-Allsopp M, Van Naarden Braun K, Doernberg NS, Benedict RE, Kirby RS & Durkin MS (2008). Prevalence of cerebral palsy in 8-year-old children in three areas of the United States in 2002: a multisite collaboration. *Pediatrics* **121**, 547–554.

Author contributions

Study conception and design: L.R.S., S.R.W., H.G.C., R.L.L. Sample collection: L.R.S., K.S.L., H.G.C. Data analysis: L.R.S. Manuscript preparation: L.R.S., R.L.L. Manuscript editing: L.R.S, K.S.L., S.R.W., H.G.C, R.L.L. All authors approved the final version for publication. This work was completed at University of California, San Diego and Rady Children's Hospital, San Diego, CA, USA.

Acknowledgements

This work was supported by grants from the National Institute of Health (AR057393), the Department of Veterans Affairs and the Department of Defense (DoD) through the National Defense Science & Engineering Graduate Fellowship (NDSEG) Program. We also acknowledge Dr Eric Edmonds for assistance collecting biopsies, Gretchen Meyer for assistance in analysis of mechanical data, Austin Carr for assistance with titin and MyHC gels, Randy Gastwirt for assistance with the hydroxyproline assay, Vera Debelynska for assistance with histology, and Shannon Bremner for technical assistance. We thank Dr. Scott Delp and Edith Arnold for making control sarcomere length calculations. The authors have no conflicts of interest regarding the publication of this work.